

An optimized pipeline for parallel image-based quantification of gene expression and genotyping after *in situ* hybridization

Tomasz Dobrzycki*¹, Monika Krecsmarik*^{1,2}, Florian Bonkhofer¹, Roger K. Patient^{1,2} and Rui Monteiro^{1,2}

1. MRC Molecular Haematology Unit, MRC Weatherall Institute of Molecular Medicine, John Radcliffe Hospital, University of Oxford, Oxford, OX3 9DS, United Kingdom
2. BHF Centre of Research Excellence, Oxford, United Kingdom

*These authors contributed equally.

Contact details:

MRC Weatherall Institute of Molecular Medicine, John Radcliffe Hospital, University of Oxford, Oxford, OX3 9DS, United Kingdom

Email: rui.monteiro@imm.ox.ac.uk

Tel: +44(0)1865222373

ABSTRACT

Recent advances in genome engineering technologies have resulted in the generation of numerous zebrafish mutant lines. A commonly used method to assess gene expression in the mutants is *in situ* hybridization (ISH). Because the fish can be distinguished by genotype after ISH, comparing gene expression between wild type and mutant siblings can be done blinded and in parallel. Such experimental design reduces the technical variation between samples and minimises the risk of bias. Applying this approach to ISH, however, requires an efficient and robust method of genomic DNA extraction from post-ISH fixed zebrafish samples to ascribe phenotype to genotype. Here we describe a method to obtain PCR-quality DNA from 95-100% of zebrafish embryos, suitable for subsequent genotyping after ISH. In addition, we provide an image analysis protocol for quantifying gene expression in the trunks of ISH-probed embryos, easily adaptable to analyse different expression patterns. Finally, we show that intensity-based image analysis enables accurate representation of the variability of gene expression detected by ISH and that it correlates well with quantitative methods like qRT-PCR. By combining genotyping after ISH and computer-based image analysis we have established a high-confidence, unbiased methodology to assign gene expression levels to specific genotypes.

INTRODUCTION

The emergence of genome engineering technologies, including zinc-finger nucleases (ZFNs)^{1,2}, transcription activator-like effector nucleases (TALENs)³ and clustered regularly interspaced short palindromic repeats (CRISPR)/Cas9⁴, has enabled zebrafish researchers to generate a wide range of mutant lines by precisely targeting genomic loci with high efficiency⁵. These methods provide alternatives to morpholino oligonucleotides (MOs), which have been used for gene knock down studies for over 15 years⁶. In the light of recent concerns regarding the reliability of phenotypes induced by MOs⁷, targeted gene knockouts have become a powerful tool to verify the transient MO phenotypes⁸ or to study genetic mutants, using MOs as a secondary tool⁹. Low-cost protocols for

DNA isolation¹⁰ and for genotyping of zebrafish embryos¹¹ have allowed faster generation and analysis of new mutant lines.

One of the most widely used methods to analyse molecular phenotypes during embryonic development is *in situ* hybridization (ISH). This technique is used to detect spatial expression patterns and tissue-specific changes in mRNA levels. Relevant protocols with several extensions have been standardised¹² and numerous validated probes are curated on the ZFIN database¹³. Using ISH to analyse MO phenotypes requires processing of the MO-treated and control samples separately, which may result in an inherent bias and an increased risk of technical variation. Lack of reported measures to reduce the risk of bias has recently been exposed in a meta-analysis of *in vivo* animal studies¹⁴. Genomic mutants offer a way to overcome these issues. Wild type and mutant embryos can be processed in one sample, assessed phenotypically in a blinded manner and then distinguished based on their genotype. This way, the technical variation between samples is minimised and phenotypic assessment is largely bias-free. A few publications have reported approaches to analyse mutant lines with ISH, using either proteinase K treatment^{9, 15} or commercial kits¹⁶ for subsequent DNA extraction. However, the efficiency of DNA extraction and genotyping methods has not been adequately demonstrated. Thus, there is a need for a powerful, efficient and fast method to analyse molecular phenotypes of newly generated zebrafish mutants with ISH.

Reporting of phenotypes has usually been confined to one representative ISH image per condition, limiting the ability to quantitatively represent the variability of the phenotype. Approaches to score the expression levels as 'high', 'medium' or 'low' by eye¹⁷⁻²⁰ are subjective and limited in how accurately they represent the effect of a knockout or a knockdown. Furthermore, visual scoring is inherently prone to poor reproducibility and low sensitivity. A more accurate way to quantitatively evaluate the change in gene expression levels involves counting the cells that contain the ISH signal²¹. However, this method is difficult to apply to compact anatomical structures, as the cell boundaries are hard to distinguish. In addition, it can be time-consuming and tedious if several

genotypes and large sample sizes need to be counted. Intensity-based image analysis using a selected region of interest (ROI) provides an objective alternative to visual scoring. Fan and colleagues have recently described a method using the ImageJ Software to quantify ISH signal intensity in mouse embryos, where measurements were taken along a straight line drawn across the developing forelimb²². Wen et al. have adapted this technique for use in the zebrafish to quantify gene expression levels in the mesoderm during early embryonic development²³. This approach can be further optimised to quantify gene expression after ISH in other regions and at other stages of the developing embryo.

Here we provide an optimised protocol for fast, inexpensive and highly efficient Hot Sodium Hydroxide and Tris (HotSHOT)-based²⁴ isolation of DNA from fixed zebrafish embryos aged 22 hours to 5 days post fertilisation for PCR and genotyping after ISH. This method is extremely reliable and allowed successful genotyping in 95-100% of the embryos. In addition, we propose a detailed step-by-step guide for gene expression intensity measurements based on modifications to the previously described quantitation methods^{22, 23}. This pipeline provides a useful tool for high-confidence, bias-free reporting of molecular phenotypes using standard ISH.

METHODS

Maintenance of zebrafish and morpholino oligonucleotide injections

All animal experiments were approved by the local ethics committee. Wild type and *runx1*^{W84X 25} fish were maintained and bred according to standard procedures¹². Embryos were collected by natural mating and staged according to morphological features²⁶ corresponding to respective age in hours or days post fertilisation (hpf or dpf, respectively). For *gpr65* knockdown, wild type one-cell stage embryos were injected with 4ng of GPR65_SP MO¹⁷.

Whole-mount in situ hybridization

ISH was carried out according to the standard lab protocol²⁷ using digoxigenin-labelled *dnmt3bb.1*⁹ and *runx1*²⁸ probes. Post hybridization, the embryos were bleached in 5% formamide/0.5% SSC/10% H₂O₂²⁹ and imaged in 100% glycerol with QImaging MicroPublisher 5.0 RTV Camera and Q-Capture Pro 7™ software (version 7.0.3), using the same exposure, magnification and illumination settings for each embryo.

DNA extraction and genotyping

Genomic DNA was isolated from 4% paraformaldehyde(PFA)-fixed embryos using the original HotSHOT protocol²⁴ (Fig. 1). Briefly, 40-75µl of lysis buffer (25mM NaOH, 0.2mM EDTA) was added directly to a PCR tube with a freshly-imaged embryo in <5µl 100% glycerol. To test the efficiency of the DNA extraction, embryos were suspended in the buffer and incubated at 95°C for 30-120 minutes, then cooled to 4°C, after which an equal amount of neutralisation buffer (40-75µl 40mM Tris-HCl) was added (see detailed Supplementary protocol). Genomic regions containing the mutated sites in the *runx1* locus were amplified with JumpStart™ REDTaq® ReadyMix™ PCR or with Phire™ Green HotStart II PCR Master Mix according to manufacturer protocols, using 5µl of DNA lysate in a 20µl reaction volume and the following primer sequences: 5'-GCTCTGGTGGGCAAAGT-3' and 5'-CATGTGTTTGGACTGTGGGG-3'. The presence of *runx1* mutations was verified by restriction fragment length polymorphism (RFLP)³⁰ with HaeII enzyme (New England Biolabs) on a 2% agarose gel, using 100bp DNA Ladder (New England Biolabs) as a reference.

Digital image analysis

Using Fiji software³¹, the images were inverted to negative and converted to 8-bit grayscale. A Region of Interest (ROI) containing the ISH expression signal in the dorsal aorta along the yolk sac extension was drawn manually for each embryo. Then a second ROI with the same shape and area was created in a region of the embryo that has a uniform intensity and does not contain any ISH staining. In this particular instance, this region was placed just above the notochord (Fig. 1). This area was used to define the background. A value for each region was then determined by measuring

the average pixel intensity. After subtracting the value of the background region from the value of the stained region, the pixel intensity of the ISH signal was assigned to each embryo (Fig. 1. and detailed Supplementary protocol).

Statistical analysis

The numbers of embryos scored as 'high', 'medium' or 'low' were tested for equal distribution among wild type, heterozygous and mutant genotypes with a contingency Chi-squared test. For digitally analysed images, the pixel intensity values were assessed for normal distribution with a Q-Q plot. Mean values (μ) of each experimental group were analysed with 2-tailed independent-samples *t*-tests with 95% confidence levels, testing for the equality of variances with a Levene's test and applying the Welch correction when necessary. For all these analyses the IBM® SPSS® Statistics (version 22) package was used. The degree of variability in each sample was assessed by calculating the coefficients of variation, defined as $\frac{s(x)}{\mu}$, with $s(x)$ being the standard deviation. The post-hoc power of the tests and required sample sizes were determined with G*Power software (version 3.0.10)³². The graphs presenting individual data points, means and \pm SD were plotted using GraphPad Prism 7.

RESULTS

ISH embryos can be efficiently genotyped with HotSHOT and JumpStart™ REDTaq® PCR

Simple and cost-effective genotyping of zebrafish embryos relies on efficient amplification of the genomic region of interest with PCR. We assessed whether variable factors, such as the length of lysis, the age of embryos or the type of DNA polymerase affected the efficiency of PCR following genomic DNA extraction from embryos after ISH using the standard HotSHOT protocol²⁴. We found that 30 minutes of incubation in 25mM NaOH at 95°C allowed unambiguous genotyping with 95-100% efficiency regardless of the stage of the embryos, from 22hpf until 5dpf (Fig. 1). Longer incubation times (60 min.) reduced the efficiency to around 85%, while incubating the samples for

120 minutes largely abolished the detection of a PCR product (data not shown). In addition, incubation of the samples overnight at 4°C after the addition of Tris-HCl improved the efficiency of PCR. When comparing two different commercially available PCR master mixes, we found the JumpStart™ REDTaq® ReadyMix™ to be on average more efficient than Phire™ Green HotStart II PCR Master Mix, although the difference between the two varied from sample to sample. We successfully applied this strategy to genotype eight different mutant lines (7 unpublished and *runx1*^{W84X} mutants) using RFLP.

Digital quantification of the ISH signal in the dorsal aorta reveals a significant decrease of dnmt3bb.1 mRNA levels in runx1^{W84X/W84X} mutants and a significant increase of runx1 expression in gpr65 morphants

To demonstrate the usefulness of our genotyping protocol in a known mutant, we imaged 130 embryos from the incross of *runx1*^{+/^{W84X}} heterozygotes, fixed at 33hpf and probed for *dnmt3bb.1* mRNA, a known downstream target of *runx1* within the haemogenic endothelium⁹ (Fig. 2A). Scoring of the images as ‘high’, ‘medium’ or ‘low’ showed a Mendelian 1:2:1 distribution of phenotypes (Supplementary Fig. 1A). We then genotyped all the imaged embryos with 100% efficiency using the above protocol and RFLP (Fig. 2B). The observed Mendelian distribution of phenotypes, resulting from the first phenotypic assessment, did not entirely correspond to the respective genotypes. While the ‘low’ phenotype was significantly overrepresented in the homozygous mutant group ($\chi^2=95.3$, d.f.=4, $p<0.001$), there was no difference in the distribution of ‘high’- and ‘medium’-expressing embryos among wild type and heterozygous fish ($\chi^2=1.35$, d.f.=1, $p>0.2$) (Supplementary Fig. 1B). For a more quantitative assessment, we independently used Fiji to digitally quantify pixel intensities of each embryo in the dorsal aorta region along the yolk sac extension prior to genotyping. This approach relied on allocating two separate ROIs to each image: one containing the staining and another containing an equal area of the embryo without any staining (Fig. 1). By subtracting the background value from the staining value, a number was assigned to each embryo.

After genotyping, we compared the signal intensity values in wild type, heterozygous and mutant embryos. While there was no significant difference between wild types and heterozygotes ($t=1.53$, d.f.=92, $p>0.1$), the *runx1* mutant embryos showed a statistically significant reduction by approximately 50% of *dnmt3bb.1* signal compared to wild types ($\mu_{wt}=54$, $\mu_{mut}=26.3$; $t=11.3$, d.f.=41, $p<0.001$) or heterozygotes ($\mu_{het}=50.1$, $\mu_{mut}=26.3$; $t=13.9$, d.f.=94, $p<0.001$) (Fig. 2C). We found that the signal intensity values in all groups were very dispersed, with high coefficients of variation (24%, 22% and 21% for wild type, heterozygote and mutant groups, respectively).

We applied the same analysis method to the images of 16 *gpr65* morphants and 16 control (uninjected) siblings probed at 29hpf for *runx1* mRNA, previously shown to be downstream of *gpr65*¹⁷. We found a significant increase of approximately 25% in pixel intensity levels of the *runx1* probe staining in *gpr65* knockdown embryos, compared to non-injected controls ($\mu_{wt}=29$, $\mu_{gpr65}=37.2$; $t=2.38$, d.f.=30, $p<0.05$) (Fig. 3). The values of the wild type embryos and the morphants showed dispersion with the coefficients of variation of 34% and 26%, respectively. The power of this *t* test to detect the difference at 0.05 level was 63%.

DISCUSSION

The HotSHOT method of genomic DNA isolation, originally designed for mouse ear notch samples²⁴, offers a fast and cost-effective way to genotype animals. While it has been used to isolate genomic DNA from PFA-fixed zebrafish samples before^{10, 33}, its efficiency in this setting had not been assessed or reported. In consequence, the method has not been widely adopted in the community and a number of research groups rely on time-consuming and more expensive DNA extraction methods involving proteinase K treatment⁹ or commercially available kits^{16, 34}. Here we report that PCR-quality DNA can be extracted from 95-100% of fixed zebrafish embryos aged from 22hpf to 5dpf with an optimised HotSHOT protocol after ISH. This DNA can be subsequently used to genotype the samples with simple, inexpensive PCR followed by a digest to detect restriction enzyme sites disrupted by the mutation, as done previously for fresh tissue³⁰. To facilitate this, mutations can be designed to target

restriction enzyme recognition sites. In fact, an online TALEN and CRISPR/Cas9 design tool Mojo Hand³⁵ readily provides restriction enzyme sites targeted by a desired mutation. While newly emerging alternatives to standard PCR and RFLP may provide a higher speed of genotyping^{36, 37}, we recommend the protocol described here for genotyping after ISH due to its high efficiency and demonstrated robustness in our hands.

Genotyping zebrafish embryos after ISH is important because it allows processing of mutant and wild type embryos in one batch, therefore limiting the technical variation between samples. In addition, expression levels of the target gene can be assessed in a non-biased way, because the embryos can be distinguished by their genotype only after phenotypic assessment. This is a powerful way to control for unconscious bias, a serious issue in *in vivo* animal research¹⁴. Assessing mRNA levels in post-ISH embryos has been performed visually, either by scoring the phenotypes into discrete groups^{17, 18, 20} or by cell counting²¹. However, these approaches are prone to subjectivity and poor reproducibility. Furthermore, visual scoring can be difficult to carry out and interpret due to expression level differences between individuals of the same genotype. Indeed, we show here that pixel intensities of the ISH signal in wild type embryos probed for the transcription factor *runx1* show high dispersion in wild type embryos with over 25% coefficient of variation (Fig. 3B and data not shown). These results indicate that the interpretation of phenotypes based purely on expected Mendelian distribution from heterozygous incrosses might be misleading. As we demonstrate, visual scoring of embryos from a heterozygous *runx1*^{+/*W84X*} incross into 'high', 'medium' and 'low' groups based on *dnmt3bb.1* expression levels gives a phenotypic Mendelian distribution of 1:2:1, which could suggest a haploinsufficiency effect. Genotyping of these embryos revealed that the vast majority of 'low'-expressing ones were indeed genetically homozygous mutant. However, both 'high'- and 'medium'-expressing embryos were distributed similarly across wild type and heterozygous fish, disproving the haploinsufficiency hypothesis. As a possible explanation for this discrepancy, we found that the signal intensity values in all three genotypes were highly dispersed, with coefficients of variation over 20%. Therefore, each ISH experiment done on embryos from a

heterozygous incross should be followed by genotyping to avoid misleading conclusions due to the variability of the ISH signal intensities in embryos of the same genotype.

We argue that the use of digital image analysis on ISH-probed samples is critical for objective, statistical demonstration of expression level changes. Here we describe a protocol based on previous studies^{22, 23} to measure gene expression intensity in the trunk region of 1-2 day old zebrafish embryos. We show that the average ISH staining intensity for *dnmt3bb.1* mRNA is significantly decreased in *runx1* mutants compared to wild type siblings, in agreement with previously reported qRT-PCR quantitation of *dnmt3bb.1* levels in whole embryos⁹. Thus, our method is robust and we suggest it should be adopted instead of less reliable visual scoring methods. It could also be used as an alternative to qRT-PCR experiments where these require larger numbers of animals and are prone to errors due to a limited number of highly reliable internal controls³⁸. Our quantification method addresses all these limitations. Furthermore, it presents a way to measure changes in expression levels in a very tissue-specific manner, which is useful in the case of genes with multiple developmental roles. We believe it will be particularly helpful for studying other genes with expression patterns that are spatially restricted, such as *gata2b*, a haematopoietic gene expressed in the ventral wall of dorsal aorta³⁹. We also propose a way to quantitatively represent variation in gene expression levels without relying on subjective and biased scoring. For instance, we could replicate the previously reported increase in *runx1* expression in *gpr65* morphants¹⁷ with our method, but we represented it in a more objective quantitative way, also allowing powerful statistical analysis. In fact, we achieved 63% power to detect a 25% increase in pixel intensity at the $p < 0.05$ level for sample sizes as small as 16 for each condition. This method of analysis also allows precise calculations of required sample sizes to achieve given power. In the presented example, 80% power would require 24 MO-injected embryos and 24 uninjected controls. Such calculations are essential in animal research⁴⁰, but they are notoriously unreported¹⁴. In addition, there is scope to automate the intensity measurements of the ISH images⁴¹, which could speed up phenotypical analysis using this method in the future.

ACKNOWLEDGEMENTS

We thank Dr Dominic Waithe from Wolfson Imaging Centre for the advice on developing the image quantification method. We thank staff members of Biomedical Services at the John Radcliffe Hospital for monitoring and feeding zebrafish. T.D. was funded by a Wellcome Trust Chromosome and Developmental Biology PhD Scholarship (#WT102345). R.M. and M.K. were funded by the British Heart Foundation (BHF IBSR Fellowship FS/13/50/30436). R.K.P. and F.B. were funded by the Medical Research Council. R.M. acknowledges support from the BHF Centre of Research Excellence (RE/13/1/30181), Oxford.

Author Disclosure Statement

No competing financial interests exist.

REFERENCES

1. Doyon Y, McCammon JM, Miller JC, Faraji F, Ngo C, Katibah GE, et al.: Heritable targeted gene disruption in zebrafish using designed zinc-finger nucleases. *Nature biotechnology*. 2008;26:702-8.
2. Meng X, Noyes MB, Zhu LJ, Lawson ND, Wolfe SA: Targeted gene inactivation in zebrafish using engineered zinc-finger nucleases. *Nature biotechnology*. 2008;26:695-701.
3. Huang P, Xiao A, Zhou M, Zhu Z, Lin S, Zhang B: Heritable gene targeting in zebrafish using customized TALENs. *Nature biotechnology*. 2011;29:699-700.
4. Hwang WY, Fu Y, Reyon D, Maeder ML, Tsai SQ, Sander JD, et al.: Efficient genome editing in zebrafish using a CRISPR-Cas system. *Nature biotechnology*. 2013;31:227-9.
5. Varshney GK, Sood R, Burgess SM: Understanding and Editing the Zebrafish Genome. *Advances in genetics*. 2015;92:1-52.
6. Nasevicius A, Ekker SC: Effective targeted gene 'knockdown' in zebrafish. *Nature genetics*. 2000;26:216-20.
7. Kok FO, Shin M, Ni CW, Gupta A, Grosse AS, van Impel A, et al.: Reverse genetic screening reveals poor correlation between morpholino-induced and mutant phenotypes in zebrafish. *Developmental cell*. 2015;32:97-108.
8. Rossi A, Kontarakis Z, Gerri C, Nolte H, Hölper S, Krüger M, et al.: Genetic compensation induced by deleterious mutations but not gene knockdowns. *Nature*. 2015;524:230-3.
9. Gore AV, Athans B, Iben JR, Johnson K, Russanova V, Castranova D, et al.: Epigenetic regulation of hematopoiesis by DNA methylation. *eLife*. 2016;5.
10. Meeker N, Hutchinson S, Ho L, Trede N: Method for isolation of PCR-ready genomic DNA from zebrafish tissues. *BioTechniques*. 2007;43:610-4.
11. Wilkinson RN, Elworthy S, Ingham PW, van Eeden FJM: A method for high-throughput PCR-based genotyping of larval zebrafish tail biopsies. *BioTechniques*. 2013;55.
12. Westerfield M: *The zebrafish book. A guide for the laboratory use of zebrafish (Danio rerio)*. 5th ed. Eugene, OR: Univ of Oregon Press; 2007.

13. Howe DG, Bradford YM, Conlin T, Eagle AE, Fashena D, Frazer K, et al.: ZFIN, the Zebrafish Model Organism Database: increased support for mutants and transgenics. *Nucleic acids research*. 2013;41:60.
14. Macleod MR, McLean A, Kyriakopoulou A, Serghiou S, de Wilde A, Sherratt N, et al.: Risk of Bias in Reports of In Vivo Research: A Focus for Improvement. *PLoS biology*. 2015;13:e1002273.
15. Zhu C, Smith T, McNulty J, Rayla AL, Lakshmanan A, Siekmann AF, et al.: Evaluation and application of modularly assembled zinc-finger nucleases in zebrafish. *Development*. 2011;138:4555-64.
16. Bresciani E, Carrington B, Wincovitch S, Jones M, Gore AV, Weinstein BM, et al.: CBF β and RUNX1 are required at 2 different steps during the development of hematopoietic stem cells in zebrafish. *Blood*. 2014;124:70-8.
17. Gao X, Wu T, Johnson KD, Lahvic JL, Ranheim EA, Zon LI, et al.: GATA Factor-G-Protein-Coupled Receptor Circuit Suppresses Hematopoiesis. *Stem cell reports*. 2016;6:368-82.
18. Genthe JR, Clements WK: R-spondin 1 is required for specification of hematopoietic stem cells through Wnt16 and Vegfa signaling pathways. *Development*. 2017;144:590-600.
19. Place ES, Smith JC: Zebrafish *atoh8* mutants do not recapitulate morpholino phenotypes. *PloS one*. 2017;12:e0171143.
20. Blaser BW, Moore JL, Hagedorn EJ, Li B, Riquelme R, Lichtig A, et al.: CXCR1 remodels the vascular niche to promote hematopoietic stem and progenitor cell engraftment. *The Journal of experimental medicine*. 2017;214:1011-27.
21. Espín-Palazón R, Stachura DL, Campbell CA, García-Moreno D, Del Cid N, Kim AD, et al.: Proinflammatory signaling regulates hematopoietic stem cell emergence. *Cell*. 2014;159:1070-85.
22. Fan Y, Richelme S, Avazeri E, Audebert S, Helmbacher F, Dono R, et al.: Tissue-specific gain of RTK signalling uncovers selective cell vulnerability during embryogenesis. *PLoS Genet*. 2015;11:e1005533.
23. Wen B, Yuan H, Liu X, Wang H, Chen S, Chen Z, et al.: GATA5 SUMOylation is indispensable for zebrafish cardiac development. *Biochim Biophys Acta*. 2017.
24. Truett GE, Heeger P, Mynatt RL, Truett AA, Walker JA, Warman ML: Preparation of PCR-quality mouse genomic DNA with hot sodium hydroxide and tris (HotSHOT). *BioTechniques*. 2000;29:52-4.
25. Jin H, Sood R, Xu J, Zhen F, English MA, Liu PP, et al.: Definitive hematopoietic stem/progenitor cells manifest distinct differentiation output in the zebrafish VDA and PBI. *Development*. 2009;136:647-54.
26. Kimmel CB, Ballard WW, Kimmel SR, Ullmann B, Schilling TF: Stages of embryonic development of the zebrafish. *Developmental Dynamics*. 1995;203:253-310.
27. Jowett T, Yan YL: Double fluorescent in situ hybridization to zebrafish embryos. *Trends Genet*. 1996;12:387-9.
28. Kalev-Zylinska ML, Horsfield JA, Flores MV, Postlethwait JH, Vitas MR, Baas AM, et al.: Runx1 is required for zebrafish blood and vessel development and expression of a human RUNX1-CBF2T1 transgene advances a model for studies of leukemogenesis. *Development*. 2002;129:2015-30.
29. Monteiro R, Pouget C, Patient R: The *gata1/pu.1* lineage fate paradigm varies between blood populations and is modulated by *tif1y*. *The EMBO journal*. 2011;30:1093-103.
30. Hruscha A, Krawitz P, Rechenberg A, Heinrich V, Hecht J, Haass C, et al.: Efficient CRISPR/Cas9 genome editing with low off-target effects in zebrafish. *Development*. 2013;140:4982-7.
31. Schindelin J, Arganda-Carreras I, Frise E, Kaynig V, Longair M, Pietzsch T, et al.: Fiji: an open-source platform for biological-image analysis. *Nature methods*. 2012;9:676-82.
32. Faul F, Erdfelder E, Lang A-G, Buchner A: G*Power 3: A flexible statistical power analysis program for the social, behavioral, and biomedical sciences. *Behavior Research Methods*. 2007;39:175-91.

33. Cooney JD, Hildick-Smith GJ, Shafizadeh E, McBride PF, Carroll KJ, Anderson H, et al.: Teleost growth factor independence (gfi) genes differentially regulate successive waves of hematopoiesis. *Developmental biology*. 2013;373:431-41.
34. Sood R, Carrington B, Bishop K, Jones M, Rissone A, Candotti F, et al.: Efficient methods for targeted mutagenesis in zebrafish using zinc-finger nucleases: data from targeting of nine genes using CompoZr or CoDA ZFNs. *PloS one*. 2013;8:e57239.
35. Neff KL, Argue DP, Ma AC, Lee HB, Clark KJ, Ekker SC: Mojo Hand, a TALEN design tool for genome editing applications. *BMC Bioinformatics*. 2012;14:1-7.
36. Lee HB, Schwab TL, Koleilat A, Ata H, Daby CL, Cervera R, et al.: Allele-Specific Quantitative PCR for Accurate, Rapid, and Cost-Effective Genotyping. *Human Gene Therapy*. 2016;27:425-35.
37. D'Agostino Y, Locascio A, Ristoratore F, Sordino P, Spagnuolo A, Borra M, et al.: A Rapid and Cheap Methodology for CRISPR/Cas9 Zebrafish Mutant Screening. *Molecular biotechnology*. 2016;58:73-8.
38. Xu H, Li C, Zeng Q, Agrawal I, Zhu X, Gong Z: Genome-wide identification of suitable zebrafish *Danio rerio* reference genes for normalization of gene expression data by RT-qPCR. *Journal of Fish Biology*. 2016.
39. Butko E, Distel M, Pouget C, Weijts B, Kobayashi I, Ng K, et al.: Gata2b is a restricted early regulator of hemogenic endothelium in the zebrafish embryo. *Development*. 2015;142:1050-61.
40. Dell RB, Holleran S, Ramakrishnan R: Sample size determination. *Ilar Journal*. 2002;43:207-13.
41. Chen S, Zhu Y, Xia W, Xia S, Xu X: Automated analysis of zebrafish images for phenotypic changes in drug discovery. *Journal of neuroscience methods*. 2011;200:229-36.

Figure 1. The overview of the method to extract DNA for genotyping zebrafish mutants after ISH

and measure the mRNA levels. Embryos collected from an incross of fish heterozygous for a mutant allele are probed for the measured gene with a standard ISH protocol. After imaging in 100% glycerol, genomic DNA is extracted using the HotSHOT protocol by adding the lysis buffer directly to the embryo in a 0.2ml PCR tube, followed by a 30min. incubation at 95°C. This DNA is used for genotyping of the embryos with PCR and restriction fragment length polymorphism (RFLP). In parallel, the images for each embryo are inverted and converted to 8-bit greyscale. ROIs containing the ISH signal and background are manually selected and measured. The measurements, assigned to corresponding genotypes, are statistically analysed.

Figure 2. Compared to wild type, *runx1* mutants have significantly reduced levels of *dnmt3bb.1*

mRNA detected by ISH. A) A representative image of a *dnmt3bb.1*-probed 33hpf embryo, showing the expression in the dorsal aorta. B) 2% agarose gel showing representative genotypes of wild type (WT), heterozygous (HET) and mutant (MUT) *runx1* embryos, distinguished by RFLP. Yellow: wild-type 214bp + 124bp bands, pink: 338bp mutant band. First lane from the left: 100bp DNA ladder. C) Pixel intensity values of *dnmt3bb.1* mRNA in wild type (N=32), heterozygous (N=62) and *runx1* mutant (N=36) embryos. The bars represent mean \pm SD. *** $p < 0.001$.

Figure 3. Compared to uninjected siblings, *gpr65* morphants have significantly increased levels of

***runx1* mRNA detected by ISH.** A) A representative image of a *runx1*-probed 29hpf embryo, showing the expression in the dorsal aorta. B) Pixel intensity values of *runx1* mRNA in uninjected control (N=16) and *gpr65* MO-injected (N=16) embryos. The bars represent mean \pm SD. * $p < 0.05$.

Fig. 1

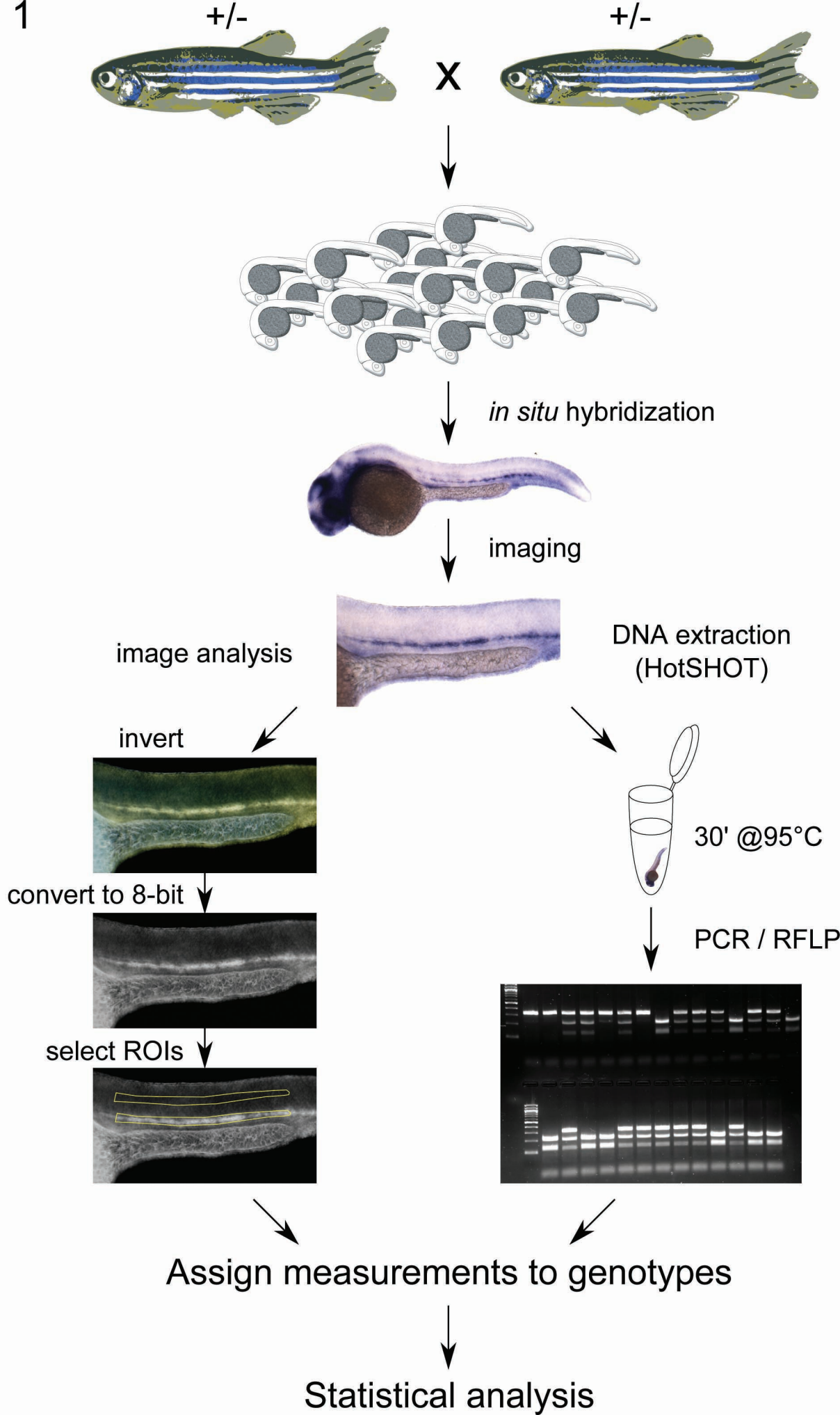


Fig. 2

